Heliyon 9 (2023) e21238

Contents lists available at ScienceDirect

Heliyon

journal homepage: www.cell.com/heliyon

Chemical, thermal and morphological properties of polybutylene succinate-waste pineapple leaf fibres composites

Mohau Justice Phiri [a,*], Julia Puseletso Mofokeng [b], Mapoloko Mpho Phiri [c], Mfiso Mngomezulu [b], Zikhona Tywabi-Ngeva [c]

[a] Department of Biotechnology & Chemistry, Vaal University of Technology, Private Bat X021, Vanderbijlpark, 1911, South Africa
[b] Department of Chemistry, University of the Free State (Qwaqwa Campus), Private Bag X13, Phuthaditjhaba, 9866, South Africa
[c] Department of Chemistry, Nelson Mandela University, P.O. Box 7700, Gqeberha, 6031, South Africa

ARTICLE INFO

Keywords:
Biodegradable polymer composites
Natural fibres
Waste pineapple leaf fibres
Thermal characteristics
Morphological properties
XRD patterns

ABSTRACT

The use of natural fibres for polymer composite applications has been widely researched due to the biodegradable and lightweight nature of natural fibres. To achieve good adhesion and compatibility between the matrix and the fibre filler, prior modification of the fibre surface via the use of various methods has been found to be effective. The natural fibres have been modified using chemical, physical, radiation, grafting and biological methods. The current study aims to evaluate the effect of sodium hydroxide-treated waste pineapple leaf fibres (PALF) content on the chemical, thermal, and morphological properties of polybutylene succinate (PBS) composites. PBS-PALF composites with fibre content ranging from 0 to 20 wt% were prepared using an internal mixer and their properties were studied using Fourier transform infrared (FTIR), X-ray diffraction (XRD), Differential scanning calorimetry (DSC), Thermogravimetric analysis (TGA) and Scanning electron microscope (SEM). The FTIR results showed no noticeable functionality differences among the composites, however, carbonyl groups from PBS polymer at ~1700 cm^{-1} and hydroxyl groups from PALF at ~3000 cm^{-1} were observed in the composites. The water absorption uptake of the composites increased with fibre content due to the hydrophilic nature of the PALF fibres and the highest water absorption percentage achieved was ~30 %. The incorporation of the fibres into the PBS matrix decreased the crystallinity of the composites as shown by the XRD peaks at $2\Theta = 22$ and 30°. SEM images of the composites with 20 wt% exhibited morphologies where the fibres protruded out from the polymer matrix, and this was ascribed to the agglomerated fibres which were poorly mixed with the matrix at the higher fibre content. Overall, the incorporation of high PALF content in the composites disrupted the crystallinity and thermal stability of the PBS matrix. The composites have potential in industrial agricultural mulching film applications due to their sustainability characteristics.

1. Introduction

Polymer composites have a wide range of applications in industries like automotive, food packaging, and construction [1–5]. Several naturally based and man-made fillers have been used to improve the mechanical, chemical, and thermal properties of the

* Corresponding author.
E-mail addresses: mohaup@vut.ac.za, mohaujphiri@gmail.com (M.J. Phiri).

https://doi.org/10.1016/j.heliyon.2023.e21238
Received 29 March 2023; Received in revised form 5 October 2023; Accepted 18 October 2023
Available online 24 October 2023

composites [6–8]. Natural fibre usage in various applications is due to its biodegradability and low-weight characteristics [9–11]. Composites derived from natural fibres have been studied extensively and waste fibre composites are assumed to be environmentally friendly since the use of such fibres reduces the pollution to the environment [9,12,13]. The advantages of using pineapple leaf fibres (PALF) in the current study are their biodegradability and hydrophilic characteristics hence they can easily degrade in the environment. Moreover, PALFs are readily available as waste materials, thus they can result in cheaper polymer composites. One of the factors that limited the application of natural fibre/polymer composites was the poor compatibility among the components with the polymer matrix [5,14–17]. As such, several surface modification methods, namely physical [11,18], biological [19,20], chemical [21–23] and grafting [24,25], have been researched and found to improve the interfacial bonding of the components of the natural fibre/polymer composites [11,18–25].

The chemical modification of natural fibres has been extensively studied for application in polymer composites [11,12,26–28]. The aim of the modification is to reduce the hydrophilic nature of the fibres to improve adhesion with the polymer matrix [14,29,30]. Sheltami et al., 2012 [31] treated Mengkuang leaves with alkali and bleaching process using 4 % sodium hydroxide (NaOH) and 17 % of $NaClO_2$ at 125 °C for 4 h and isolated fibres were further treated with 60 % of H_2SO_4 at 45 °C for 45 min. The Soxhlet extraction results showed that after treatment with alkali, cellulose increased whereas hemicellulose decreased, and partial removal of lignin was reported after a repeated bleaching process. SEM images confirmed the partial removal of lignin and showed that fibres had reduced diameters. The increased crystallinity of the treated fibres was confirmed by XRD experiments.

Soundrapandian et al., 2021 [32] used untreated and treated Palmyra leaves to produce polyester resin composites with fibres that have different lengths, long and short. They modified the fibres with 5 % NaOH solution at room temperature for a period of 30 min and rinsed them with 2.5 % HCl and distilled water. The surface-treated fibres were smoother due to the removal of waxes, oil, and some of the lignin material. SEM images showed similar behaviour between composites with long and short untreated fibres as there were pull-out of fibres from the epoxy resin matrix which resulted in poor interfacial bonding; however, the observation was less noticed for the NaOH-treated fibres.

Chen et al., 2021 [33] prepared recycled high-density polyethylene composites having 40, 60 and 80 wt% of rice husk fibre content. From the water absorption results, they observed that the percentage of retained water in the composites increased with higher fibre content and longer immersion time due to the hydrophilic nature of the fibres. There was a slight increase in the thermal stability of the composites with the highest fibre content, 80 wt%. In another study, Oliver-Ortega et al., 2020 [34] fabricated polylactic acid composites filled with 10–35 wt% fibre content of kraft softwood. The impact strength of the composites was found to decrease with an increase in fibre content and the results of SEM analysis were used to confirm this behaviour since the morphologies of the composites showed agglomeration of fibres. This suggested that there was poor interaction among the composite components. Enciso et al. [35] prepared low-density polyethylene composites having 15–40 wt % of flax fibres and they have found that the increase in the fibre content resulted in decreased crystallinities of the composites. The studied literature showed that the effect of chemical modification and fibre loading on the overall properties of the composites depends on the strength of the modifier, pre-treatment steps, content of the natural fibres and polymer matrix.

The current study aims to prepare completely biodegradable polymer composites with waste PALF as a natural fibre and optimise composite properties for possible application in the agricultural mulching industry. The fibres will be modified with 10 wt% sodium hydroxide solution and various amounts of fibre will be compounded with polybutylene succinate (PBS) polymer matrix using an internal mixer operated at a temperature of 120 °C. Composites with different PALF contents ranging from 0 to 20 wt% will be analysed and characterised for chemical composition, thermal, crystallinity and morphological properties using various techniques, namely, FTIR, DSC, TGA, XRD and SEM. The comprehensive information from the PBS-PALF composite results will be used to evaluate the effect of fibre content on the overall properties of the PBS composites and determine their possible final applications in the agricultural mulching industry.

2. Experimental procedure

2.1. Materials and chemicals

A biodegradable polymer, polybutylene succinate, with a melt flow index of 12 g/10min and a density of ~1.26 g/cm^3 was supplied by the Sasol Company, South Africa. The waste PALF was supplied by the local pineapple farmers and the dried fibres were ground to 18 mesh particle size before use in the composite formulations. The estimated amounts of cellulose, lignin and hemicellulose were ~50 %, ~30 % and ~20 %, respectively.

2.2. Modification of pineapple leaf fibres with sodium hydroxide

PALF (50 g) was soaked in 10 % NaOH solution and the mixture was heated at 60 °C on a hot plate with stirring at 10 rpm for 2 h. The modified PALF was separated via filtration followed by 2 washes of acetic acid (10 %) to neutralize the residual NaOH and finally rinsed three times with distilled water. The modified PALF samples were dried overnight in the oven set at a temperature of 30 °C.

2.3. Preparation of the polybutylene succinate (PBS)-PALF composites

The formulations of the PBS-PALF composites were prepared according to Table 1 with the fibre content ranging from 0 to 20 wt%. The composites of PBS polymer and PALF were mixed in an internal mixer at 120 °C and 40 rpm as illustrated in Fig. 1. The mixing

procedure was carried out for 4 min and the PBS-PALF composites were kept at room temperature for further analyses.

2.4. Characterization of the PBS-PALF composites

2.4.1. Thermal analysis

TA instrument (DSC model Q200) was used to investigate the thermal behaviour of the PBS-PALF composites as illustrated in Fig. 1. 5.0 mg of each sample was weighed into aluminium pans and the heating rate was set at 10 °C/min in the temperature range from 40 to 200 °C. Three heating cycles were applied for each measurement and the analysis was undertaken under a nitrogen atmosphere at 50 mL/min. The thermal decomposition of the composites was studied with the use of a thermogravimetric analyzer. About 6.0 mg of each composite was weighed into a platinum pan and heated from 40 to 600 °C at a rate of 10 °C/min and nitrogen flow rate of 50 mL/min.

2.4.2. Fourier transform infrared (FTIR) analysis

The chemical composition and functional groups of the PBS-PALF composites were examined by FTIR. Attenuated total reflectance instrument, FTIR-Bruker Tensor, with a spectral range of 4000 cm^{-1}–400 cm^{-1}, and 64 scans were performed using a resolution of 8 for the measurements.

2.4.3. Water absorption analysis

For the water absorption study, samples of about 0.50 g were weighed and dried in the oven at pre-set at the temperature of approximately 30 °C for 24 h. The samples were subsequently swollen in distilled water over a period of 3 weeks (21 days). The samples were taken out of the water, patted dry with a paper towel, weighed periodically, and placed back in the water for the duration of the analysis. The percentage of water absorption (WA %) was calculated according to Eq. (1); where M_i and M_f are the initial and final masses, respectively.

$$WA\ (\%) = \frac{M_f - M_i}{M_i} \times 100 \tag{1}$$

2.4.4. X-ray diffraction (XRD) analysis

XRD results of the PBS-PALF composite samples were collected using Bruker 8 advanced XRD system and the X-ray generator was operated at a voltage of 40 kV with a detector using 1D mode. The scan mode was continuous PSD fast with a Ni filter (0.02 mm) and the slit size was 0.6 mm. The 2theta (2Θ) angles were selected in the range of 15–50° with an increment of 0.01945°.

2.4.5. Field emission scanning electron microscopy (FE-SEM)

The SEM analyses of the PBS-PALF composite samples were examined by a scanning electron microscope (SEM) instrument, model Tescan Vega 3. Before the analyses, the composite samples were coated with carbon material, and they were placed on aluminium stubs with carbon conductive tape. The scanning measurements were done with a voltage of 20 kV and a magnification of 500 μm for all the analyses.

3. Results and discussion

3.1. FTIR analysis

The chemical composition of the PBS-PALF composite samples was determined by FTIR and the results are depicted in Fig. 2. The spectra for all the samples look similar as there were no observable differences among the composites. This is attributed to PBS and PALF having similar structures, where each has hydroxyl, carbonyl, and hydrocarbon groups in their structure. The peak at 1713 cm^{-1} is due to the carbonyl group on the backbone of the PBS polymer, which gets intense with the addition and increase in the content of pineapple leaf fibre. The intensity of this peak increased with the increasing amount of PALF in the composites. The peaks around 2900-2800 cm^{-1} are a result of protons of methylene groups on the PBS polymer and hydrocarbon groups in PALF material while the peak around 3427 cm^{-1} is associated with the hydroxyl groups from the cellulose and hemicellulose components in the fibre.

3.2. Water absorption analysis

The water absorption properties of the composites were evaluated over a period of 21 days for the possible application as

Table 1
Formulations of the PBS-PALF composites.

Sample Name	Mass of PBS (g)	Mass of PALF (g)
PBS-PALF-0	53.1	0.0
PBS-PALF-5	49.3	2.6
PBS-PALF-10	46.7	5.2
PBS-PALF-15	44.1	7.8
PBS-PALF-20	41.5	10.4

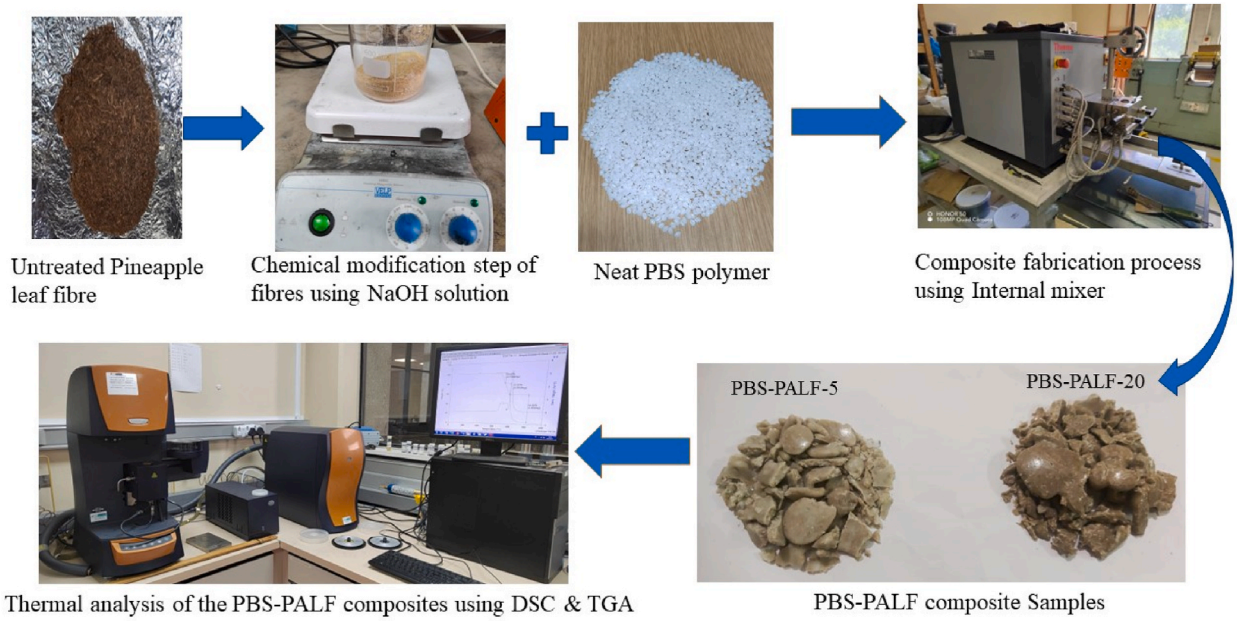

Fig. 1. Process flow diagram for modification of PALF, fabrication and characterization of the PBS-PALF composites.

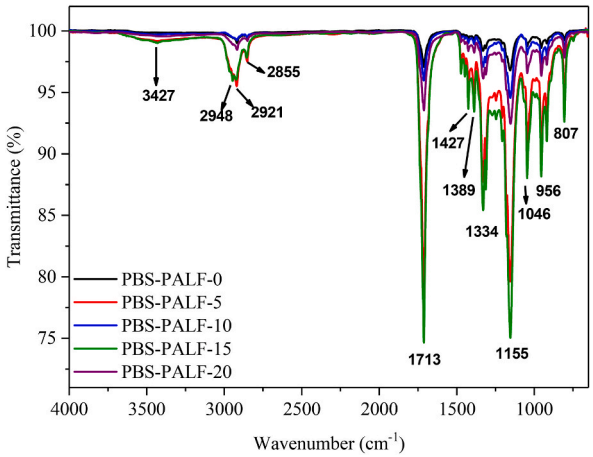

Fig. 2. FTIR analysis of the PBS-PALF composites with a fibre content of 0–20 wt%.

agricultural mulching film and the results are shown in Fig. 3. It is clear that PBS is totally hydrophobic since it did not absorb any moisture/water for the duration of the test. Adding pineapple leaf fibre to the PBS resulted in composites absorbing water. Generally, results showed that all the composite samples exhibited water absorption values below 30 %. The percentage of the water absorbed was observed to increase with an increase in the PALF content and as a function of time per individual composite material, with samples, PBS-PALF-15 and PBS-PALF-20, exhibiting the highest values of equilibrium water absorption. This behaviour was expected due to the hydrophilic nature of the cellulose and hemicellulose components in PALF since they contain hydroxyl functional groups. The expectation is that lower water absorption percentage values, below 15 %, will result in the mulching film that will conserve both water and soil moisture content because at this water absorption level, the composites present minimum water permeability. On the other hand, higher water absorption percentage values are recommended to facilitate fast degradation of the natural fibre-based composites [36].

3.3. Thermal analysis

The thermal properties of the neat PBS and composites were analysed by Differential scanning calorimetry (DSC) and Thermogravimetric analyser (TGA) and the results are presented in Fig. 4 (DSC), 5 (TGA) as well as Table 2 with thermal degradation

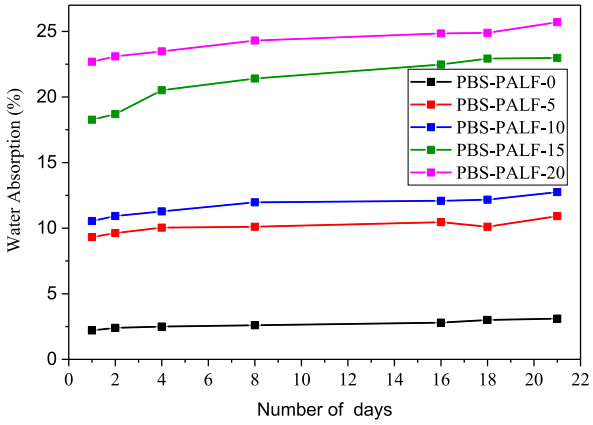

Fig. 3. Water absorption results of the PBS-PALF composites with a fibre content of 0–20 wt%, and the measurements were taken over three weeks.

temperatures. Starting with DSC, one peak was observed at ~110 °C for all the samples and it was associated with the melting of the PBS polymer matrix. The only disparity between the composites and neat PBS was that the height of the melting peak increased with increasing PALF content in the composites. It is known that the melting enthalpy of the sample is related to the height and area of its peak [29], thus, the incorporation of the fibre at high contents disrupted the crystallinity of the PBS polymer. There was also a broadening of peaks with higher fibre contents which signified an increase in the range and size distribution of the crystallites, and this could be due to heterogeneous nucleation brought by the fibre into PBS polymer chains. The heat flow increased with the addition of fibre into the PBS composites, implying that the composite samples with a higher amount of PALF content have increased stiffness and require high energy consumption during their fabrication process. The sample's torque was found to increase with an increase in fibre content in the composites during the melt mixing step. From our previous work [29], the increase in fibre content resulted in composites with increased stiffness, which in turn affected the rheological properties of the sample. This means that the composites containing lower fibre content will require less processing time and lower energy requirements.

Fig. 5 shows the thermal degradation results of the PBS-PALF composites, and three sets of peaks were observed. The peaks at ~120 °C are assigned to low-boiling point components such as water, oil and waxes, and the set of peaks at ~240–300 °C is assigned to the thermal degradation of cellulose, hemicellulose, and lignin in the fibre material. Additionally, an increase in the height of the peaks at ~240–300 °C was observed as the percentage of PALF increased in the composites. The last set of peaks at ~300–500 °C is assigned to the degradation of PBS polymer and there is a decrease in the peak height as the amount of PBS also decreases in the composites, there is no shift in the thermal degradation temperature of the composites.

The second and the last degradation steps seem to be merging since the polymer starts degrading while the degradation of cellulose is in progress. The footprints of PBS and PALF components in the TGA results insinuate that there was a lack of interaction between the fibre and the polymers, though their co-degradation at temperatures around 300 °C may indicate partial miscibility. The assumption that could be made is that the incorporation of PALF fibres in the polymer composites lowered the onset degradation temperature of the PBS polymer matrix. But overall, the maximum degradation temperature of the composites remained at a constant temperature.

The thermal decomposition results of the PBS-PALF composites are presented in Table 2. The qualitative information about the general thermal stabilities of the material is provided by T5 and T50 values which were extracted from the TGA curves [29,37]. T5

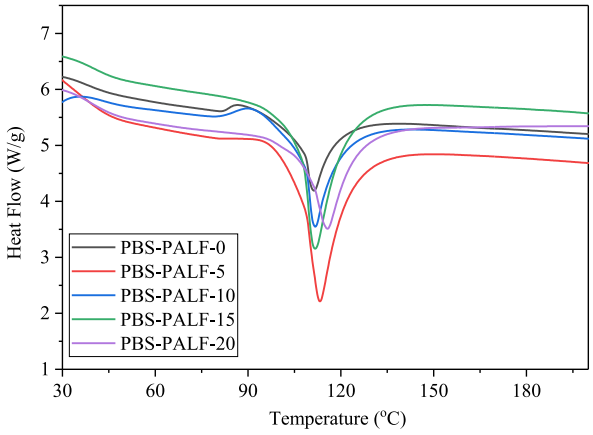

Fig. 4. DSC results of the PBS/PALF composites with a fibre content of 0–20 wt% (Endotherm down).

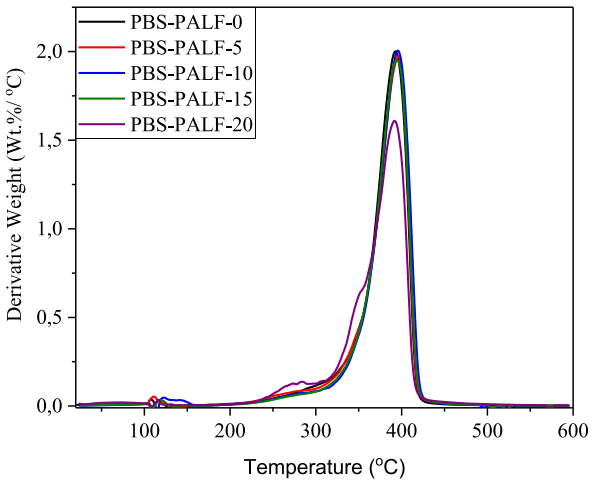

Fig. 5. TGA results of the PBS-PALF composites with a fibre content of 0–20 wt%.

Table 2
Thermal characteristics of the PBS-PALF composites as analysed by TGA.

Sample Name	T5 (°C)[a]	T20 (°C)[a]	T50 (°C)[a]	Residue (%)
PBS-PALF-0	290	356	384	1.88
PBS-PALF-5	292	361	387	1.91
PBS-PALF-10	278	355	385	2.53
PBS-PALF-15	289	361	387	4.95
PBS-PALF-20	266	345	383	8.27

[a] Thermal degradation temperature at different weight loss percentages. T5, T20 and T50 are temperature values at 5, 20 and 50 % weight loss, respectively.

values decreased upon increasing the amount of fibre in the composites, suggesting that there were more volatile components in the PALF material. T50 values provide information about the maximum degradation temperature of the composites [29]. The results showed that the composites have similar values of ~385 °C and this is related to the PBS polymer matrix. The percentage of the residue increased with the fibre content in the composites, further suggesting that the PBS matrix is more thermally stable than the PALF component. The overall thermal properties showed that the fabricated composites can withstand extremely hot weather conditions as their thermal degradation temperature values are above normal environmental conditions.

3.4. X-ray diffraction (XRD) analysis

The degree of dispersion (intercalation and/or exfoliation) of the PALF in the PBS was studied by using X-ray diffraction (XRD). This was achieved by analysing the position, shape, and intensity as well as the change in lamellar spacing (d-spacing) of the diffraction

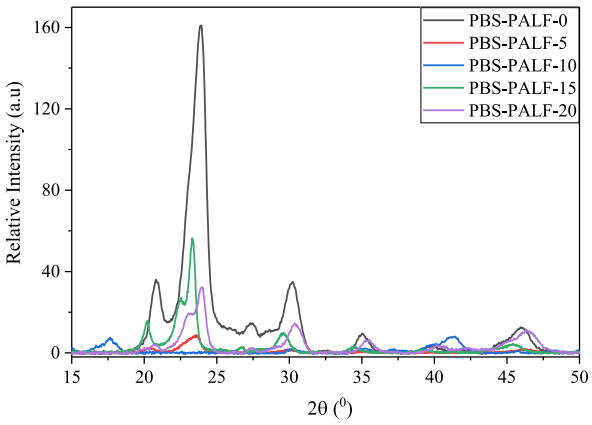

Fig. 6. XRD results of the PBS-PALF composites with a fibre content of 0–20 wt%.

peaks. Fig. 6 depicts the XRD patterns of neat PBS and its composites with PALF at various contents. The PBS presents four overlapping crystalline peaks in the range of $2\theta = \sim 20–32^{\circ}$, with the main sharp peak at $2\theta = 22.5^{\circ}$. The sharp and narrow peaks at $2\theta = \sim 20$ and ~ 22.5 are assigned to different crystal planes of the α-form of PBS crystal structure and the peak at $2\theta = 35$ is assigned to the β-form of PBS crystal structure which can only occur under sample stress deformation [38]. The broad and wider peaks at $2\theta = \sim 35$, ~ 40, and ~ 46 are assigned to the amorphous form of PBS structure resulting from either the extended side chains on the main polymer backbone or the percentage of monomer content [39]. The XRD of the neat PBS polymer exhibited an intense sharp peak, indicating that PBS has a high degree of crystallinity. This peak was present in all composite samples and there was no significant shift observed, the only observable difference was a height decrease. This could be due to the presence of PALF fibres inhibiting the alignment of polymer chains and hence decreasing the degree of crystallinity in the composites. The observed decrease in crystallinity was confirmed by SEM analysis as illustrated in Fig. 7. Agglomerated fibres were noticeable from the SEM images at higher fibre content.

3.5. Morphology of neat PBS and its composites with PALF

Fig. 7 presents the SEM results of neat PBS and its composites with NaOH-treated PALF. Neat PBS, Fig. 7(a), shows a smooth surface with periodic spherical objects, which might be a result of bubbles that formed, or granules that remained in the melt during mixing. The PBS-PALF composites with lower fibre content (5 and 10 wt%), Fig. 7(b and c), exhibited well-dispersed filler within the matrix, which reflects good adhesion among composite components. Good interaction is evidenced by the absence of gaps between the fibres and the polymer matrix, and no fibre protruding out of the matrix. At high fibre content, there was not enough surface on the polymer to accommodate the fibre and there were cavities observed within 15 and 20 wt% PBS-PALF composites, see Fig. 7(d and e). As shown in Fig. 7(e), the 20 wt% PALF sample showed agglomeration of the filler and some fibres sticking out of the PBS polymer matrix. In return, the strong fibre-to-fibre interaction caused agglomeration at higher PALF fibre content. These morphological behaviours at high fibre content translate to high water absorption percentage values as the incompatibility between the composite components creates unoccupied interphases or empty pores to allow the penetration of water into the composites.

4. Conclusion

The study investigated the chemical, thermal and morphological properties of PBS polymer composites filled with PALF fibre in the range from 0 to 20 wt%. The composites were fabricated using an internal mixer at 120 °C, a processing time of 4 min and analysed by using different analytical techniques. During the mixing process, the flow behaviour of the composites was monitored, and the melt flow was found to increase with an increase in fibre content. These results were confirmed by DSC measurements which indicated that the heat flow of the composite samples increased with fibre content. The FTIR results showed that the intensity of the carbonyl peak at $\sim 1700\ cm^{-1}$ from the PBS polymer backbone was slightly affected by the increase of fibre content in the PBS-PALF composites. The water absorption percentage increased up to ~30 % for the composite with the highest fibre content due to the presence of hydroxyl groups from the cellulose and hemicellulose components of the PALF fibre. This behaviour is essential for the final application of the composite material. It has previously been shown that natural fibre-based composites can degrade by either hydrolytic degradation or biodegradation in the soil and under compost environmental conditions [40].

The thermal properties of the composites were examined to determine the thermal degradation behaviour of the samples. TGA results indicated that the thermal stability of the composite samples remained unchanged and was not affected by the addition of the fibres since the PALF material thermally degraded earlier at 300 °C as compared to the PBS polymer matrix which had maximum thermal degradation peak at ~385 °C. This shows that the fabricated composite samples had the potential to withstand hot weather conditions. Results obtained from XRD showed that the intensities of the α-form of PBS crystalline structure peaks at $2\theta = \sim 20$ and $\sim 22.5^{\circ}$ decreased with an increase in the fibre content and this indicated that the incorporation of the fibre into the composites disrupted the crystallinity of the PBS polymer chain.

SEM images showed that there was an agglomeration of the fibres in the composite samples, PBS-PALF-15 and PBS-PALF-20, and there was also fibre phasing out for the sample with the highest fibre content, 20 wt%. These results confirmed decreased crystallinity as observed in the XRD patterns of the composites. However, samples with lower fibre content showed good adhesion behaviour between the PBS matrix and PALF. Overall, the fabrication and characterization of the polymer composites with water absorption percentages of less than 30 % were successful and these composites could be used as mulching films for agricultural applications. The developed composites significantly decrease the economic costs associated with the production of mulching films from pure polymer materials by incorporating free and readily available agricultural waste in the form of PALF from local farmers. This in turn will contribute to the elimination of waste disposal.

Data availability statement

The data generated and analysed in the current study is included in the article, however, all the raw data will be made available upon request.

CRediT authorship contribution statement

Mohau Justice Phiri: Conceptualization, Data curation, Formal analysis, Investigation, Methodology, Project administration, Supervision, Validation, Visualization, Writing – original draft, Writing – review & editing. **Julia Puseletso Mofokeng:** Data curation,

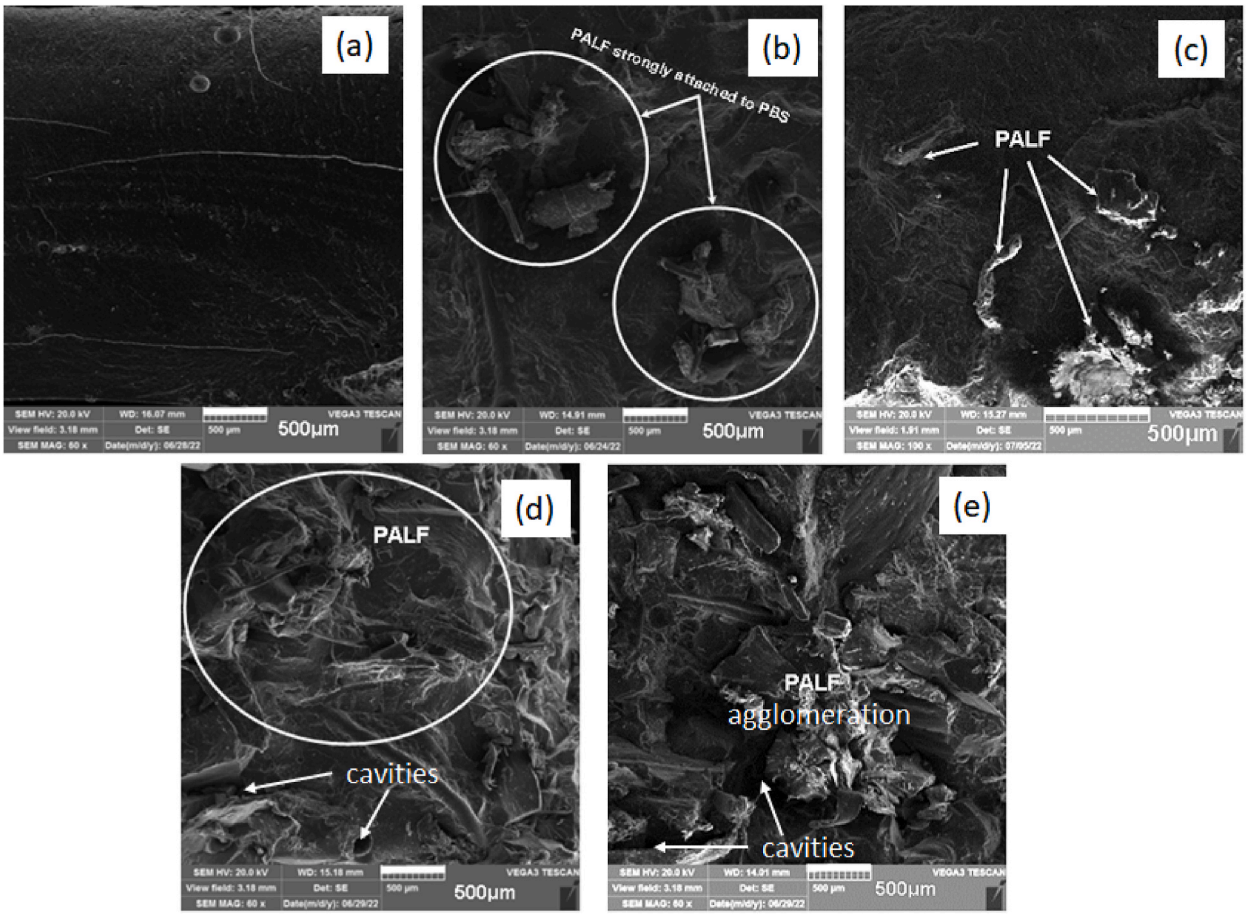

Fig. 7. Morphological results of the PBS-PALF composites with a fibre content of 0–20 wt% using 500 µm magnification, (a) PBS-PALF-0, (b) PBS-PALF-5, (c) PBS-PALF-10, (d) PBS-PALF-15 and (e) PBS-PALF-20.

Formal analysis, Investigation, Methodology, Writing – original draft, Writing – review & editing, Validation, Visualization. **Mapoloko Mpho Phiri:** Data curation, Formal analysis, Methodology, Validation, Writing – original draft, Writing – review & editing, Investigation. **Mfiso Mngomezulu:** Formal analysis, Resources, Writing – original draft, Writing – review & editing. **Zikhona Tywabi-Ngeva:** Project administration, Resources, Writing – original draft, Writing – review & editing.

Declaration of competing interest

The authors declare that they have no known competing financial interests or personal relationships that could have appeared to influence the work reported in this paper.

Acknowledgements

The present research work was financially supported by the Vaal University of Technology, the University of Free State and Nelson Mandela University.

References

[1] S. Kazemi Najafi, Use of recycled plastics in wood plastic composites – a review, Waste Manag. 33 (2013) 1898–1905, https://doi.org/10.1016/j.wasman.2013.05.017.
[2] Y. Li, Effect of woody biomass surface free energy on the mechanical properties and interface of wood/polypropylene composites, J. Adhes. Sci. Technol. 28 (2014) 215–224, https://doi.org/10.1080/01694243.2013.835951.
[3] J. Zhao, X.-M. Wang, J.M. Chang, Y. Yao, Q. Cui, Sound insulation property of wood–waste tire rubber composite, Compos. Sci. Technol. 70 (2010) 2033, https://doi.org/10.1016/j.compscitech.2010.03.015. –8.
[4] M.Z.R. Khan, S.K. Srivastava, M.K. Gupta, A state-of-the-art review on particulate wood polymer composites: processing, properties and applications, Polym. Test. 89 (2020), 106721, https://doi.org/10.1016/j.polymertesting.2020.106721.

[5] C.M. Chan, L.-J. Vandi, S. Pratt, P. Halley, D. Richardson, A. Werker, et al., Composites of wood and biodegradable thermoplastics: a review, Polym. Rev. 58 (2018) 444–494, https://doi.org/10.1080/15583724.2017.1380039.

[6] K.L. Pickering, M.G.A. Efendy, T.M. Le, A review of recent developments in natural fibre composites and their mechanical performance, Compos Part A Appl Sci Manuf 83 (2016) 98–112, https://doi.org/10.1016/j.compositesa.2015.08.038.

[7] M. Chougan, S.H. Ghaffar, M.J. Al-Kheetan, M. Gecevicius, Wheat straw pre-treatments using eco-friendly strategies for enhancing the tensile properties of bio-based polylactic acid composites, Ind. Crops Prod. 155 (2020), 112836, https://doi.org/10.1016/J.INDCROP.2020.112836.

[8] J.J. Kenned, K. Sankaranarayanasamy, J.S. Binoj, S.K. Chelliah, Thermo-mechanical and morphological characterization of needle punched non-woven banana fiber reinforced polymer composites, Compos. Sci. Technol. 185 (2020), 107890, https://doi.org/10.1016/j.compscitech.2019.107890.

[9] M.J. John, R.D. Anandjiwala, Recent developments in chemical modification and characterization of natural fiber-reinforced composites, Polym. Compos. 29 (2008) 187–207, https://doi.org/10.1002/pc.20461.

[10] N.H. Sari, S. Suteja, A. Fudholi, A. Zamzuriadi, E.D. Sulistyowati, P. Pandiatmi, et al., Morphology and mechanical properties of coconut shell powder-filled untreated cornhusk fibre-unsaturated polyester composites, Polymer (Guildf) 222 (2021), 123657, https://doi.org/10.1016/j.polymer.2021.123657.

[11] R. Ahmad, R. Hamid, S.A. Osman, Physical and chemical modifications of plant fibres for reinforcement in cementitious composites, Adv. Civ. Eng. 2019 (2019), 5185806, https://doi.org/10.1155/2019/5185806.

[12] K.J. Wong, B.F. Yousif, K.O. Low, The effects of alkali treatment on the interfacial adhesion of bamboo fibres, Proc. Inst. Mech. Eng., Part L 224 (2010) 139–148, https://doi.org/10.1243/14644207JMDA304.

[13] T. Alsaeed, B.F. Yousif, H. Ku, The potential of using date palm fibres as reinforcement for polymeric composites, Mater. Des. 43 (2013) 177–184, https://doi.org/10.1016/j.matdes.2012.06.061.

[14] Y. Cao, S. Shibata, I. Fukumoto, Mechanical properties of biodegradable composites reinforced with bagasse fibre before and after alkali treatments, Compos Part A Appl Sci Manuf 37 (2006) 423–429, https://doi.org/10.1016/j.compositesa.2005.05.045.

[15] Y. Fan, C. Mei, Y. Liu, L. Mei, Effect of surface free energy of wood-flour and its polar component on the mechanical and physical properties of wood-thermoplastic composites, Rev. Adv. Mater. Sci. 33 (2013) 211–218.

[16] S. Yi, S. Xu, Y. Fang, H. Wang, Q. Wang, Effects of matrix modification on the mechanical properties of wood–polypropylene composites, Polymers 9 (2017) 712, https://doi.org/10.3390/polym9120712.

[17] Z. Jun, W. Xiang-ming, C. Jian-min, Z. Kai, Optimization of processing variables in wood–rubber composite panel manufacturing technology, Bioresour. Technol. 99 (2008) 2384–2391, https://doi.org/10.1016/J.BIORTECH.2007.05.031.

[18] P.K. Jena, J.R. Mohanty, S. Nayak, Effect of surface modification of vetiver fibers on their physical and thermal properties, J. Nat. Fibers 19 (2022) 25–36, https://doi.org/10.1080/15440478.2020.1726249.

[19] A. Flitsch, E.N. Prasetyo, C. Sygmund, R. Ludwig, G.S. Nyanhongo, G.M. Guebitz, Cellulose oxidation and bleaching processes based on recombinant Myriococcum thermophilum cellobiose dehydrogenase, Enzym. Microb. Technol. 52 (2013) 60–67, https://doi.org/10.1016/j.enzmictec.2012.10.007.

[20] Y. Li, K.L. Pickering, Hemp fibre reinforced composites using chelator and enzyme treatments, Compos. Sci. Technol. 68 (2008) 3293–3298, https://doi.org/10.1016/j.compscitech.2008.08.022.

[21] S. Sathish, N. Karthi, L. Prabhu, S. Gokulkumar, D. Balaji, N. Vigneshkumar, et al., A review of natural fiber composites: extraction methods, chemical treatments and applications, Mater Today Proc 45 (2021) 8017–8023, https://doi.org/10.1016/J.MATPR.2020.12.1105.

[22] M. Arsyad, R. Soenoko, The effects of sodium hydroxide and potassium permanganate treatment on roughness of coconut fiber surface, MATEC Web of Conferences: EDP Sciences 204 (2018), 05004, https://doi.org/10.1051/matecconf/201820405004.

[23] A. Mohammed, D. Bachtiar, M. Rejab, S. Hasany, Effect of potassium permanganate on tensile properties of sugar palm fibre reinforced thermoplastic polyurethane, Indian J. Sci. Technol. 10 (2018) 1–5, https://doi.org/10.17485/ijst/2017/v10i7/111453.

[24] Y. Song, Q. Wang, G. Han, H. Wang, H. Gao, Effects of two modification methods on the mechanical properties of wood flour/recycled plastic blends composites: addition of thermoplastic elastomer SEBS-g-MAH and in-situ grafting MAH, J. Res. 21 (2010) 373–378, https://doi.org/10.1007/s11676-010-0084-1.

[25] L. Mosia, M.J. Phiri, K. Garde, S.P. Hlangothi, Effect of ethylene-1-butene as a compatibilizer for the optimization of wood flour and ground tyre rubber in polypropylene composites, Journal of Composites Science 6 (2022) 220, https://doi.org/10.3390/jcs6080220.

[26] M. Jonoobi, J. Harun, A. Shakeri, M. Misra, K. Oksman, Chemical composition, crystallinity and thermal degradation of bleached and unbleached kenaf bast (Hibiscus cannabinus) pulp and nanofiber, Bioresources 4 (2009) 626–639, https://doi.org/10.15376/BIORES.4.2.626-639.

[27] H. Burrola-Núñez, P.J. Herrera-Franco, D.E. Rodríguez-Félix, H. Soto-Valdez, T.J. Madera-Santana, Surface modification and performance of jute fibers as reinforcement on polymer matrix: an overview, J. Nat. Fibers 16 (2019) 944–960, https://doi.org/10.1080/15440478.2018.1441093.

[28] M. Das, D. Chakraborty, Influence of alkali treatment on the fine structure and morphology of bamboo fibers, J. Appl. Polym. Sci. 102 (2006) 5050–5056, https://doi.org/10.1002/app.25105.

[29] M.J. Phiri, M.M. Phiri, K. Mpitso, S.P. Hlangothi, Curing, thermal and mechanical properties of waste tyre derived reclaimed rubber–wood flour composites, Mater. Today Commun. (2020), 101204, https://doi.org/10.1016/j.mtcomm.2020.101204.

[30] B.M. Cherian, A.L. Leão, S.F. de Souza, S. Thomas, L.A. Pothan, M. Kottaisamy, Isolation of nanocellulose from pineapple leaf fibres by steam explosion, Carbohydr. Polym. 81 (2010) 720–725, https://doi.org/10.1016/J.CARBPOL.2010.03.046.

[31] R.M. Sheltami, I. Abdullah, I. Ahmad, A. Dufresne, H. Kargarzadeh, Extraction of cellulose nanocrystals from mengkuang leaves (Pandanus tectorius), Carbohydr. Polym. 88 (2012) 772–779, https://doi.org/10.1016/J.CARBPOL.2012.01.062.

[32] E. Soundrapandian, P.V. Kumar, G.S. Kumar, S. Jagan, M.M. Raj, Investigation of mechanical properties of natural fiber reinforced polymer composites, Mater Today Proc 45 (2021) 8029–8035, https://doi.org/10.1016/J.MATPR.2021.01.084.

[33] R.S. Chen, M.H. Ab Ghani, S. Ahmad, M.A. Tarawneh, S. Gan, Tensile, thermal degradation and water diffusion behaviour of gamma-radiation induced recycled polymer blend/rice husk composites: experimental and statistical analysis, Compos. Sci. Technol. 207 (2021), 108748, https://doi.org/10.1016/j.compscitech.2021.108748.

[34] H. Oliver-Ortega, Q. Tarrés, P. Mutjé, M. Delgado-Aguilar, J.A. Méndez, F.X. Espinach, Impact strength and water uptake behavior of bleached kraft softwood-reinforced PLA composites as alternative to PP-based materials, Polymers 12 (2020) 2144, https://doi.org/10.3390/polym12092144.

[35] B. Enciso, J. Abenojar, M.A. Martínez, Influence of plasma treatment on the adhesion between a polymeric matrix and natural fibres, Cellulose 24 (2017) 1791–1801, https://doi.org/10.1007/s10570-017-1209-x.

[36] X.-B. Gu, Y.-N. Li, Y.-D. Du, Biodegradable film mulching improves soil temperature, moisture and seed yield of winter oilseed rape (Brassica napus L.), Soil Tillage Res. 171 (2017) 42–50, https://doi.org/10.1016/j.still.2017.04.008.

[37] A.A. Moosa, F. Kubba, M. Raad, A.A.S. Ramazani, Mechanical and thermal properties of graphene nanoplates and functionalized carbon-nanotubes hybrid epoxy nanocomposites, Am. J. Mater. Sci. 6 (2016) 125–134, https://doi.org/10.5923/j.materials.20160605.02.

[38] K.J. Ihn, E.S. Yoo, S.S. Im, Structure and morphology of poly(tetramethylene succinate) crystals, Macromolecules 28 (1995) 2460–2464, https://doi.org/10.1021/ma00111a045.

[39] L. Aliotta, M. Seggiani, A. Lazzeri, V. Gigante, P. Cinelli, A brief review of poly (butylene succinate) (PBS) and its main copolymers: synthesis, blends, composites, biodegradability, and applications, Polymers 14 (2022) 844, https://doi.org/10.3390/polym14040844.

[40] M. Vert, I Dos Santos, S. Ponsart, N. Alauzet, J.-L. Morgat, J. Coudane, et al., Degradable polymers in a living environment: where do you end up? Polym. Int. 51 (2002) 840–844, https://doi.org/10.1002/pi.903.